ORIFICES FLOW SATURATION IN OIL HYDRAULIC APPLICATIONS

Pietro Marani[1]*, Massimo Martelli[1], Silvia Gessi[1], Cesare Dolcin[2]

[1]*CNR-IMAMOTER, Via Canal Bianco, 28, 44124, Italy*
[2]*WALVOIL SpA, Via Adige, 13/D, 42124, Reggio Emilia, Italy*
*Corresponding author: Tel.: +39 0532 735 611, E-mail address: p.marani@imamoter.cnr.it

ABSTRACT

Even though the orifice is the simplest and most common control component in fluid power systems and cavitation is an already well-established topic in the scientific literature, the flow choking or saturation effect is largely overlooked in the common engineering practice. Most of the times the phenomenon is completely ignored, unless the peculiar hissing noise is observed at the test rig, giving a hint that something wrong is happening in the hydraulic system. Even then, the focus is just on the possible component damage induced by strong cavitation, while the functional implications – in terms of flow characteristic – are neglected.

The objective of the paper is to study the phenomenon of flow saturation in hydraulic orifices to assess the formulation of the different critical cavitation numbers and cavitation indexes available from literature. For this reason, a full factorial design of experiments (DOE) is performed to determine the influence of three factors: orifice size, fluid temperature and upstream pressure. The testing is carried out on 5 orifice sizes at 3 different temperatures and 5 different upstream pressure levels. In each test, the downstream pressure is changed from 0 to the upstream pressure level, to sweep the available Δp range, both ascending and descending. In the results section an analysis of the experimental results is drawn, proposing a correlation between the critical cavitation index and the factors considered in the DOE.

To the authors' knowledge, no systematic analysis, as the one here proposed, currently exists in literature for mineral oil applications.

Keywords: Cavitation, Flow Saturation

1. INTRODUCTION

Although flow through orifices is the bread and butter of fluid power, the fact that the flow passing through an orifice actually presents an upper limit or a saturation is largely overlooked by the community of technicians and engineers.

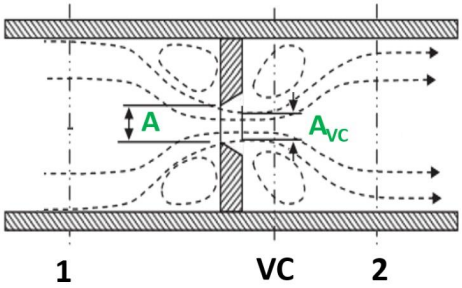

Figure 1: Classical orifice schematic

Looking at the fluid power scientific production, as stated in [1], the literature on this topic appears insufficient in terms of fundamental and applied knowledge of cavitating flow and numerically quite limited compared to the large body of research covering cavitation in flows through orifices, nozzles and Venturi tubes, often targeting real-world applications like piping systems, fuel injectors, cooling systems.

According to the most accepted explanation, the flow characteristic is quadratic until the onset of cavitation, i.e. when pressure at the vena contracta drops below the vaporization pressure (p_v). Below this threshold, and as pressure drop further increases, an increasing fraction of liquid evaporates creating the two-phase mixture. When the liquid sonic speed is reached, the fully choked flow condition is achieved, in this condition the flow rate can't increase any more i.e. flow saturation is reached; a further increase in

pressure differential will intensify the phenomenon, with flow remaining primarily in vapour phase ("flashing" condition) [2].

The release of dissolved gas (air) can also occur near the inception of cavitation, while the vaporization of the fluid, characterized by the typical hiss sound, is the dominant phenomenon during actual cavitation flow choking [1, 2, 3].
In [3] an interesting theoretical framework for the study of cavitating flow in orifices is provided.

Flow rate can be written as:

$$Q = C_d A \sqrt{\frac{2(p_1 - p_2)}{\rho}} \tag{1}$$

or

$$Q = C_c A \sqrt{\frac{2(p_1 - p_{vc})}{\rho}} \tag{2}$$

Cavitation happens when the pressure at vena contracta drops below vapour pressure, i.e. basically when Equation 3 is true:

$$C_d\sqrt{2(p_1 - p_2)} = C_c\sqrt{2(p_1 - p_v)} \tag{3}$$

Knowing the values of the discharge and contraction coefficients it would be theoretically easy to predict cavitation, but unfortunately they show variations from classical formulation due to geometry parameters and fluid properties.

Several cavitation indexes are proposed with the aim of predicting cavitation, the most significant formulae found in literature are C_{I1} [3, 4, 5, 6], C_{I2} [1, 2], C_{I3} [7], C_{I4} [3, 8].

$$C_{I1} = \frac{2(p_2 - p_v)}{\rho v^2} \approx \frac{2p_2}{\rho v^2} \tag{4}$$

$$C_{I2} = \frac{p_1 - p_v}{p_1 - p_2} \approx \frac{p_1}{p_1 - p_2} \tag{5}$$

$$C_{I3} = \frac{2(p_1 - p_2)}{\rho v^2} \tag{6}$$

$$C_{I4} = \frac{p_2 - p_v}{p_1 - p_2} \approx \frac{p_2}{p_1 - p_2} \tag{7}$$

where $v = \frac{Q}{A}$.

As shown in Equations 4, 5, 7, hydraulic fluids have negligible vapour pressures, so that this term can be safely be ignored with respect to upstream and downstream pressures.

We can note that cavitation index 1 is the mathematic representation of the ratio between the static pressure opposing to cavitation and the dynamic pressure tending to produce it, then the lower the index is, the higher the likelihood of cavitation.

Another comment can be done on the fact that the previous equations are not independent, in fact cavitation index 4 can be obtained by subtracting C_{I2} to one, C_{I1} can be obtained by multiplying C_{I2} by the square of the discharge coefficient and finally C_{I3} is the ratio of C_{I1} to C_{I4}.

The geometries of the orifice considered in this paper can be categorized as long orifice since the ratio of length to diameter is greater than 1.5, in this case, as discussed in reference [1], the flow is reattached downstream to the vena contracta region but before the exit from the orifice. From the practical side, it can be noted that most of the commercial available orifices fall into the above category of long orifices.

2. TEST METHODS

A test rig was assembled in the laboratory at Walvoil Test Department according to the ISO 4411 standard [9], in compliance with the recommended distance between the connection ports and the component under test (**Figure 2**).
The pump P supplies the circuit with an ISO VG-46 hydraulic oil. The orifice inlet pressure is kept constant via pressure relief valve V1, while electro-proportional pressure relief valve V2 controls the outlet pressure. Four measurements are acquired during the testing: inlet and outlet pressure (p_1 and p_2), flow rate through the orifice (Q) and fluid temperature (T), see **Table 1** for the details of the sensors used.

Table 1: List of sensors acquired

Design ation	Sensor type	Full Scale	Overall Precision
p_1	Thin film press. transducer	600 bar	±0,3% F. S.
p_2	Thin film press. transducer	600 bar	±0,3% F.S.
T	Semiconductor temp. transducer	-40°C 120°C	±1,5% F.S.
Q	Gear flow meter	40 l/min	±0,3% reading

A specific pipe was built including a seat for a drilled pad (**Figure 3**). The 4 mm long orifices were manufactured taking care to provide an almost square entry, being the chamfers size less than 0.01 mm.

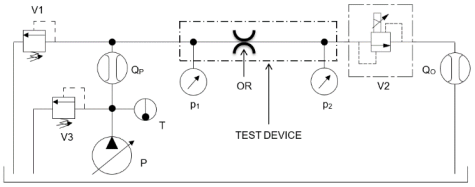

Figure 2: Test circuit

In each test, p_1 was set at a fixed nominal value, while p_2 was slowly varied from the maximum allowed pressure to the minimum and back in order to determine the flow characteristic $Q = Q(\Delta p)$.

A first full factorial design of experiments (DOE) was performed (**Table 2**) to determine the influence of three factors: orifice size (D), fluid temperature (T) and upstream pressure (p_1). The testing was carried out on 5 orifices sizes at 3 different temperatures and 5 different upstream pressure levels. Since the pad length is constant, to have additional insight of the problem additional tests were carried out with reduced orifice depth.

Table 2: Parameters of DOE

Parameter	Values	UoM
D	0.50 - 0.75 - 1.05 - 1.33 - 1.72	mm
p_1	100 – 150 – 200 – 250 - 300	bar
T	30 – 40 – 60 – 80	°C

As mentioned before, 40 additional tests were carried out at reduced orifice length, in particular tests on two additional orifices of ϕ 0.75 x 2.3 mm and of ϕ 0.75 x 2.6 mm were carried out at the 5 considered upstream pressure levels and 4 temperatures.

An important factor is the fluid, whose properties are listed below (**Table 3**).

Table 3: Fluid properties

Property	standard	Value	UoM
Viscosity ISO class	ISO 3448	VG 46	-
Density at 20°C	ASTM D 1298	869	kg/m^3
Kinematic viscosity at 0°C	ASTM D 445	552.5	cSt
Kinematic viscosity at 40°C	ASTM D 445	43.1	cSt
Kinematic viscosity at 100°C	ASTM D 445	6.83	cSt
Viscosity index	ASTM D 2270	112	-
Vapour pressure	-	<0.5	bar

3. EXPERIMENTAL RESULTS

20 tests for each orifice were carried out (5 upstream pressures by 4 temperatures), the result can be clustered by temperature, obtaining five steady flow characteristics, corresponding to five upstream pressure levels. An example of these results is shown in **Figure 4**.

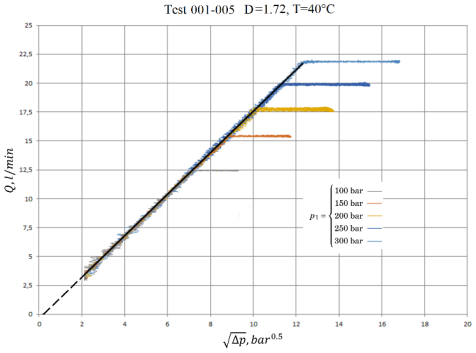

Figure 4: Flow characteristics (D = 1.72 mm, T = 40°C)

The Results, of which **Figure 4** provides a representative sample, highlight interesting properties:

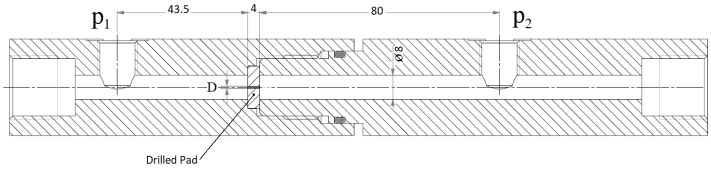

Figure 3: Test pipe with drilled pad and measurement ports

- The non-saturated flow rate characteristics at different upstream pressure overlap almost perfectly and they substantially comply with the quadratic rule.
- The flow rate becomes constant after a specific value of pressure drop is reached, clearly confirming the presence of cavitation and flow saturation.
- The characteristics show almost no hysteresis, thus it is quite easy to identify the incipient flow saturation condition and a critical cavitation index.

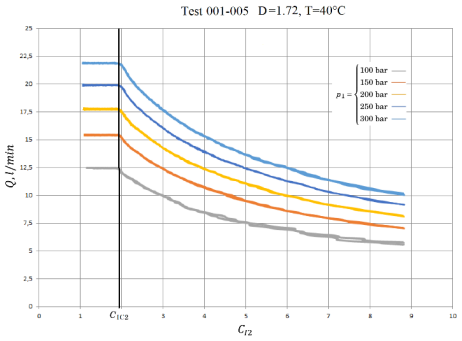

Figure 5: Cavitation index C_{I2} (D = 1.72 mm, T = 40°C)

With regard to the last observation, it is interesting to note as the hysteresis phenomenon is very relevant in particular works [3], while in other it was not observed or considered [1, 2, 4, 5]. This fact is absolutely worth investigating, and the opinion of the authors is that this discrepancy could be caused by the application air content, the type of fluid and the specific component geometry.

Since in a previous paper [1] the authors had used index C_{I2}, this index was the first one to be used.

Plotting the flow rate as a function of C_{I2} calculated from the experimental data gives a pretty clear representation of the transition from no saturation to saturation. A clear threshold separating these two distinct phases can be determined, then is it possible to define the critical cavitation index C_{IC2} as the value of the cavitation index at the boundary between saturation and no saturation flow.

Figure 5 shows a very distinct critical cavitation index that takes approximately the same value in all the tests showed, carried out at different inlet pressures and constant temperature.

4. ANALYSIS OF RESULTS

The great amount of data available from 140 tests were aggregated and sorted for diameter, temperature and upstream pressure.

4.1. DOE Results

The first results presented are referred to the full factorial DOE of the following parameters: diameter, temperature, upstream pressure, for a total 100 tests. In this case the orifices were manufactured by drilling a pad of a constant length of 4 mm.

Table 4: Sample of aggregated data

#	D [mm]	T [°C]	P_1 [bar]	C_{IC2} [-]	C_{IC5} [-]
1	1.72	32.4	98.2	1.889	2.820
2	1.72	32.6	151.0	1.932	2.815
3	1.72	31.6	199.7	1.935	2.785
4	1.72	32.6	250.7	1.929	2.804
5	1.72	32.7	299.6	1.942	2.776
6	1.72	40.7	99.4	1.912	2.846
7	1.72	39.8	150.5	1.943	2.828
8	1.72	40.3	200.9	1.958	2.820
9	1.72	40.3	250.7	1.988	2.832
10	1.72	40.9	301.1	2.000	2.803
11	1.72	60.7	100.1	1.958	2.843
12	1.72	57.6	149.6	1.995	2.822
13	1.72	60.5	201.0	1.943	2.806
14	1.72	60.4	251.4	2.019	2.811
15	1.72	58.8	304.5	1.946	2.784
16	1.72	79.5	99.8	2.008	2.825
17	1.72	80.8	150.7	2.066	2.802
18	1.72	80.9	204.0	2.061	2.785
19	1.72	78.2	250.7	2.046	2.784
20	1.72	77.9	302.2	1.978	2.733
21	1.33	30.7	100.8	1.477	2.169
22	1.33	30.9	151.7	1.526	2.135
23	1.33	32.4	201.7	1.582	2.139
24	1.33	31.6	250.5	1.611	2.125
25	1.33	32.3	302.1	1.631	2.119
26	1.33	39.8	101.9	1.572	2.138
27	1.33	40.4	151.0	1.595	2.137
28	1.33	40.2	203.4	1.619	2.136
29	1.33	41.0	251.3	1.645	2.123
30	1.33	40.6	299.0	1.638	2.108
31	1.33	60.9	100.6	1.624	2.125
32	1.33	61.1	149.9	1.630	2.133
33	1.33	59.8	199.6	1.662	2.124
34	1.33	58.6	249.2	1.691	2.117
35	1.33	61.2	300.3	1.687	2.101

36	1.33	80.3	101.6	1.692	2.122
37	1.33	80.8	149.3	1.704	2.109
38	1.33	81.2	198.9	1.686	2.096
39	1.33	78.9	247.7	1.714	2.086
40	1.33	79.5	300.7	1.705	2.081

Looking at **Table 4** representing a sample of the final table, and considering the calculated values of critical cavitation index 2 it is possible to note a large standard deviation. Aggregating the data by diameter it was found that σ=4.8% for diameter 1.72 and σ=4.8% for diameter 1.33. This can be graphically displayed in **Figure 6** and it basically means that the chosen index has low accuracy in predicting cavitation, in particular if the temperature is varied.

A possible explanation for the dispersion of C_{IC2} might be the fact that the discharge coefficient of a short orifice is almost independent from the temperature, while in case of a long orifice, characterized by reattached flow, it is affected by the viscosity and the temperature.

Considering the full spectrum of C_{IC2} for all orifice diameters (corresponding to the complete version of **Figure 6**, not shown here for simplicity), a clear trend is determined. For any given diameter, as T increases, the vertical offset of the $C_{IC2} = f(\Delta p)$ curve increases, whilst its steepness decreases, in other words the curve moves up and becomes flatter.

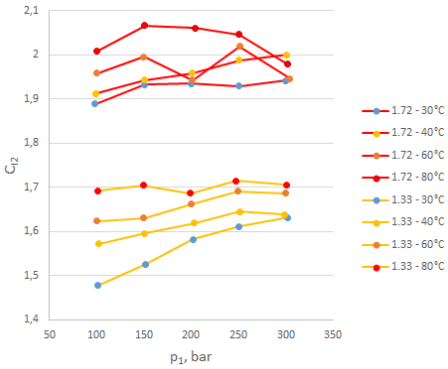

Figure 6: Critical cavitation index C_{IC2} (D = 1.72 mm, D = 1.33 mm)

The observations confirmed that the discharge coefficient calculated from the experiments highlight a sensible variation with respect to temperature. Moreover, considering that the denominator of Equation 5 represents the dynamic pressure generated by the fluid velocity, a new formula is proposed by replacing the pressure drop with a kinetic term depending on the mean velocity of fluid passing through the orifice.

$$C_{I5} = \frac{2(p_1 - p_v)}{\rho v^2} \approx \frac{2p_1}{\rho v^2} \qquad (6)$$

Formula (6) is coherent with the discussion [11] in reference to paper [12] by Cunningham who reported that pressure drop (p_1 - p_2) can be a poor approximation of the jet dynamic pressure. Consequently, he proposed the upstream to vena contracta differential pressure ($p_1 - p_{vc}$) as a more logical choice.

Critical cavitation index 5 has been calculated for each diameter highlighting a better accuracy in predicting the saturation (σ = 2.6% for diameter 1.72 and σ = 2.0% for diameter 1.33). The lower dispersion of the critical cavitation indexes 5 can be appreciated from **Figure 7** which basically is a zoom-in of the complete map of critical cavitation index 5 calculated for all tests, shown in **Figure 8**.

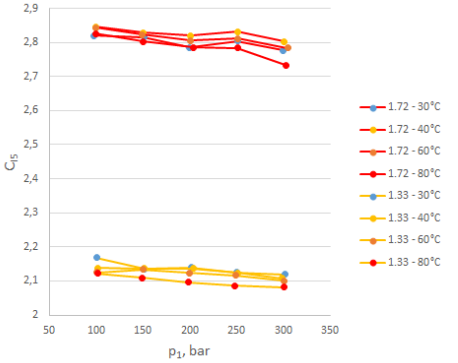

Figure 7: Critical cavitation index C_{IC5} (D = 1.72 mm, D = 1.33 mm)

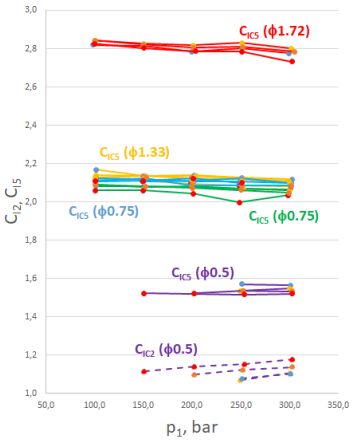

Figure 8: Critical cavitation index C_{IC5} for all the full factorial DOE

Looking at **Figure 8** is it possible to note that some points are missing for diameter 0.5. To explain this remark it is necessary to observe the critical cavitation index 2 at diameter 0.5, which is very near to unity. That is, the orifice will saturate when the pressure drop is near to the inlet pressure or, in other terms, when the downstream pressure is near to zero. Since the test rig has a minimum achievable pressure, because of the characteristics of the control valves at the orifice outlet (V2 on **Figure 2**), it was not possible to reach the saturation for all tests.

Another remark can be done on the fact that the cavitation index 5 show a small variation for each diameter but is quite difficult to find a relationship between diameter and critical cavitation index. In fact, the mean value of the index for the central values of diameter considered (D = 0.75, 1.05, 1.33) are almost overlapped while on the other hand C_{IC5} mean value is considerably lower for 0.5 mm diameter and higher for 1.72 mm.

The distribution of critical cavitation indexes is far from linear with respect to geometry parameters such as diameter or flow area.

An attempt to gain a better insight on the phenomenon has been made by considering the length of the orifice. In fact, since the pad has a constant width, the L/D parameter i.e. the ratio between length and diameter increases at decreasing diameters.

The influence of the L/D ratio on flow is thoroughly investigated in literature [10, 13], and in particular, its influence on the discharge coefficient is known, thus it is reasonable to expect a remarkable effect of L/D on the critical cavitation index.

Speaking of numbers, the L/D parameter is respectively 2.33 for ϕ 1.72, 3.01 for ϕ 1.33, 3.81 for ϕ 1.05, 5.33 for ϕ 0.75, and 8 for ϕ 0.5 mm diameter.

4.2. Additional Tests with reduced Orifice Length

In order to address the doubts which have arisen in the previous paragraph, two additional pads were prepared with reduced width, specifically an orifice of ϕ 0.75 x 2.3 mm (L/D = 3.07) and an orifice of ϕ 0.5 x 2.6 mm (L/D = 5.26).

The new orifices were tested according to the previous methods, at the same inlet pressure and at the same temperature levels.

As for the previous test batch, the critical cavitation indexes 5 show an extremely low variability.

The results of these tests are presented in **Figure 9** including also the previous results of orifice ϕ 0.5 (L/D = 8, purple lines), ϕ 0.75 (L/D = 5.33, light blue lines), ϕ 1.33 (L/D = 3.01, yellow lines).

We can couple the results for L/D matching ϕ 0.75 x 2.3 mm to ϕ 1.33 x 4 mm (blue and yellow) characterized by L/D ≈ 3 recording that the critical cavitation index 5 decreases as the diameter increases, at constant L/D ratio. On the other hand, looking at the couple ϕ 0.5 x 2.3 mm to ϕ 1.33 x 4 mm (L/D ≈ 5) we could come up with the diametrically opposite conclusion.

Observing the effect of L/D at constant diameter [ϕ 0.5 x 2.6 mm, ϕ 0.5 x 4 mm] and [ϕ 0.75 x 2.3 mm, ϕ 0.75 x 4 mm] we get a similar discrepancy. In fact, in the first couple ϕ 0.5) C_{I5} slightly decreases as the L/D ratio decreases, on the other hand, for ϕ 0.75 the index increases.

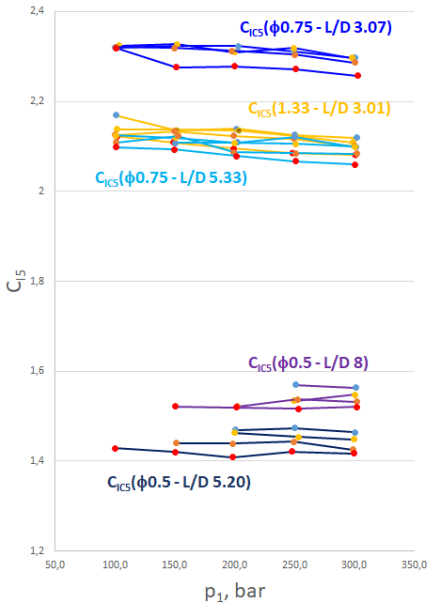

Figure 9: Comparison of critical cavitation indexes C_{I5} for different orifice lengths.

We can then conclude that even if the C_{IC5} values show a good internal consistency, it is not possible to identify a clear trend relating geometry parameters to the critical cavitation index from this set of data.

5. CONCLUSION AND OUTLOOK

A full factorial DOE was performed to study cavitation in hydraulic orifices of constant length taking into account diameter, temperature and upstream pressure. It was observed that:

- The cavitation is reached at a specific value of pressure drop, after this threshold the flow saturates (remains constant), almost no hysteresis was observed in the tests, .
- The cavitation index can be defined in different ways, a definition based on the ratio between the upstream pressure and fluid velocity proved to be an effective marker for the cavitation, dependent only from the geometry.
- The cavitation indexes based on the ratio of pressure drop and upstream/downstream pressure are less effective because they suffer from a strong dependence on temperature.
- An explicit function which relates orifice geometry to cavitation index was not found, nevertheless it was found that both diameter and length/diameter ratio influence the critical cavitation index but unfortunately the function is clearly not linear.

Starting from this study, actions on various fronts can be put in place to increase the knowledge on orifice cavitation:

- Additional testing, with particular attention to the effect of geometry parameters such as L/D.
- CFD methods can be trained with the large amount of data to get a better insight of micro-phenomena and to further explore additional cases.

Finally, cavitation is unanimously recognized as a harmful event to be prevented as much as possible because of the potential damage of components. However, the conditions for flow saturation discussed in this paper are similar to those found in current fluid power circuits, thus many components are potentially exposed to it. The fact that this allegedly may concern not only the orifices but also the valves in general from the point of view of authors represent a good point to put more effort on the topic of cavitating flows.

NOMENCLATURE

A	Orifice area
A_{vc}	Area at vena contracta
C_c	Contraction coefficient
C_d	Discharge coefficient
C_{Ij}	j-th orifice cavitation index
C_{ICj}	j-th orifice critical cavitation index
D	Orifice diameter
L	Orifice length
p_1	Orifice upstream or input pressure
p_2	Orifice downstream or output pressure
p_v	Fluid vapour pressure
p_{vc}	Vena contracta pressure
Q	Volumetric flow rate
T	Fluid temperature (upstream)
v	Orifice average flow velocity
ρ	Fluid density
σ	Standard deviation

REFERENCES

[1] Martelli, M., Gessi, S., Massarotti, G.P., Marani, P., Zarotti, G.L. (2017) On Peculiar Flow Characteristics in Hydraulic Orifices, ASME/BATH Symposium on Fluid Power and Motion Control, Sarasota, USA, 2017 FPMC2017-4313

[2] Ebrahimi, B., He, G., Tang, Y., Franchek, M., Liu, D., Pickett, J., Springett, F., and Franklin, D. (2017) Characterization of High-Pressure Cavitating Flow through a Thick Orifice Plate in a Pipe of Constant Cross Section. Int. J. Thermal Sciences 114, pp. 229-240

[3] Pearce, I.D., Lichtarowicz, A. (1971) Discharge performance of long orifices with cavitating flow, in: Proc. Second Fluid Power Symposium, January 1971, Guildford Paper D2, University of Surrey, 1971, pp. D2-13–D2-35

[4] Yan, Y., Thorpe, R.B. (1990) Flow Regime Transitions Due to Cavitation in the Flow through an Orifice. Int. J. Multiphase Flow, Vol. 16, No. 6, pp. 1023-1045.

[5] Koivula, T. (2000) On Cavitation in Fluid Power. Proc. 1st FPNI-PhD Symposium, Hamburg, Germany, pp. 371-382.

[6] Johnson, R.W. [Edited by] (2000) The Handbook of Fluid Dynamics. CRC Press LLC and Springer-Verlag GmbH, Chapter 20. ISBN 3-540-64612-4

[7] Brinkhorst, S., von Lavante, E., Wendt, G. (2016) Experimental and Numerical Investigation of the Cavitation-Induced Choked Flow in a Herschel Venturi-Tube. Flow Measurement and Instrumentation 54, pp. 56-67

[8] Castillo, M. (1993) An Analysis of Cavitation Activity at Orifices of the FFG-7 Seawater Piping System. MRL Technical Note MRL-TN-637. Department of Defence, Australia

[9] International Standard (2008). ISO 4411:2008. Hydraulic fluid power – Valves – Determination of pressure differential/flow characteristics.

[10] Lichtarowicz, A., Duggins, R. K., Markland, E. (1965) Discharge coefficients for incompressible non-cavitating flow through long orifices, J Mech Eng Sci, 1965, 7, 210–219

[11] Cunningham, R. G., Discussion: “Cavitation Inception in Spool Valves”, 1981, ASME J. Fluids Eng., 103, pp. 575–576

[12] Martin, C. S., Medlarz, H., Wiggert, D. C., and Brennen, C., Cavitation Inception in Spool Valves, 1981, ASME J. Fluids Eng., 103, pp. 564–575

[13] Idelchik, I.E. (1994) Handbook of hydraulic resistance, - 3rd Edition, CRC Press, ISBN: 0-8493-9908-4, p.222.